Numerical Investigation of the Performance and Transport Phenomena of a Proton-Exchange Membrane Fuel Cell with a Wavelike Gas Flow Channel Design

Jenn-Kun Kuo,[1] Cai-Wan Chang-Jian,[2] Cha'O-Kuang Chen[3]

[1]*Graduate Institute of Greenergy Technology, National University of Tainan, Tainan 700, Taiwan*
[2]*Department of Mechanical and Automation Engineering, I-Shou University, Kaohsiung 840, Taiwan*
[3]*Department of Mechanical Engineering, National Cheng Kung University, Tainan 70101, Taiwan*

Received 20 August 2007; accepted 23 June 2008
DOI 10.1002/app.29024
Published online 30 October 2008 in Wiley InterScience (www.interscience.wiley.com).

ABSTRACT: This article investigates the performance of a proton-exchange membrane fuel cell (PEMFC) with a novel wavelike gas flow channel. Numerical simulations have been performed to investigate the effect of the wavelike channel profile on the gas flow characteristics, temperature distribution, electrochemical reaction efficiency, and electrical performance. The simulation results show that compared to a conventional straight gas flow channel, the wavelike channel increases the fuel flow velocity, enhances the transport through the porous layer, and improves the temperature distribution. As a result, the PEMFC has improved fuel utilization efficiency and superior heat-transfer characteristics. Furthermore, the results show that the wavelike gas flow channel yields a higher PEMFC output voltage and improves the maximum power density by approximately 32.5%. © 2008 Wiley Periodicals, Inc. J Appl Polym Sci 111: 1440–1448, 2009

Key words: catalysts; electrochemistry; simulations

INTRODUCTION

Proton-exchange membrane fuel cells (PEMFCs) are regarded as a viable power source for a variety of applications. The requirements for compactness, high power density, high performance, good electrical stability, and low cost have led to the optimization of many aspects of PEMFCs. Several PEMFC models have been presented in recent years. Bernardi and Verbrugge[1,2] and Springer et al.[3] proposed one-dimensional models that provide a good preliminary foundation for more advanced PEMFC modeling. The two-dimensional models presented by Nguyen et al.[4] assume that oxygen transport is driven by diffusion alone and neglect the effects of the gas diffusion layer (GDL)[5] and the gas flow field. Hence, the practical applicability of the models is somewhat limited. Recent years have seen a significant increase in the power densities, reliability, and electrical performance of fuel cells. However, the underlying physics of the transport mechanism in a fuel cell, which involves coupled fluid flow, heat and mass transfer, and an electrochemical reaction, remain poorly understood. Accordingly, researchers have increasingly adopted the use of computational fluid dynamics simulations to model PEMFCs to obtain deeper insights into their transport mechanisms and performance characteristics.

A variety of PEMFC gas flow channel configurations have been proposed, including serpentine channels, multiple parallel channels, and interdigitated channels. The GDL forms one sidewall of the fuel channel in a PEMFC, and hence its morphology affects the transport of the reactant gas from the channel to the catalyst surface and must be taken into account. Conventional PEMFCs have straight gas flow channels. However, Kuo and Chen[6,7] proposed the use of gas flow channels with a novel wavelike form to improve the PEMFC performance. Their results showed that the unique channel design improved the uniformity of the velocity and temperature distributions within the channel and reduced the included angle between the dimensionless velocity vector and the temperature gradient, thereby improving the heat-transfer characteristics of the fuel cell.

This study presents a detailed numerical investigation of the velocity, temperature, and gas concentration distributions within the wavelike gas flow channel. Additionally, the study compares the electrical performance of a PEMFC with wavelike gas flow channels with that of a PEMFC with conventional straight gas flow channels.

Correspondence to: J.-K. Kuo (jkkuo@mail.nutn.edu.tw).
Contract grant sponsor: National Science Council of Taiwan; contract grant number: NSC 96-2221-E-006-MY3.

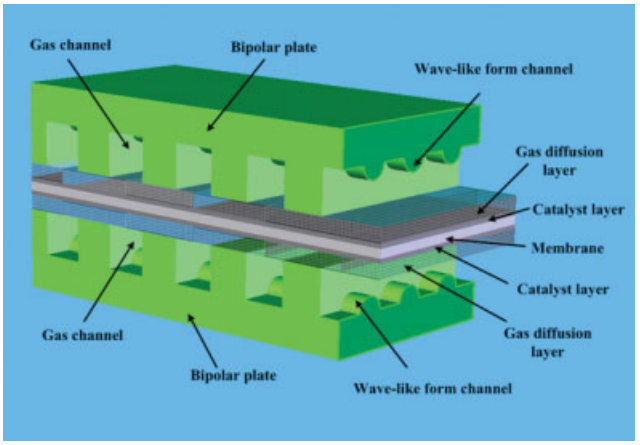

Figure 1 Schematic representation of the PEMFC. [Color figure can be viewed in the online issue, which is available at www.interscience.wiley.com.]

PEMFC MODEL

The simulations performed in this study are based on a steady-state, single-phase, multispecies, two-dimensional mass-transfer model of a PEMFC. Figure 1 presents a three-dimensional solid-rendered schematic illustration of the fuel cell. As shown, the fuel cell comprises anode and cathode flow channels with wavelike profiles, two GDLs made of a porous material (carbon paper), two catalyst layers (CLs), and a proton-exchange membrane. The geometric and physical parameters employed in these simulations are summarized in Table I.[3,8] Note that some minor parameters are omitted from this table, but they can be found in the literature.[9–13] The operating pressure and temperature are 1 atm and 323 K, respectively. The simulations assume that the anode is supplied with humidified hydrogen with a mass fraction of 70%/30% H_2/H_2O. The cathode side is fed with saturated air with a mass fraction of 21%/79% O_2/N_2. The N_2 gas is considered to be inert and serves as a diluent. An assumption is made that the hydrogen reactant gas enters the gas flow channel normal to the channel cross section. The following additional assumptions are also made:

1. The gas mixture is an incompressible, ideal fluid.
2. The Reynolds number of the fluid is less than 200, and the flow is laminar.
3. The GDL, the CL, and the membrane are all isotropic and homogeneous, and they are characterized by high permeability and a uniform porosity.
4. The electrochemical reaction is governed by Butler–Volmer kinetics.
5. The water byproduct of the electrochemical reaction at the cathode side is in a vapor state.
6. The membrane is impervious to the reactant gases.
7. The fuel cell geometry is periodic in the x-axis direction.

The governing equations are identical for both the wavelike channel and the conventional straight channel. In developing the model of the wavelike channel, it is assumed that the fuel cell geometry is periodic in the x direction. Figure 2 shows the computational model constructed for the wavelike channel. For computational efficiency, the computational domain is divided into seven separate layers: the upper wavelike channel, the anode GDL, the anode CL, the membrane, the cathode CL, the cathode GDL, and the lower wavelike channel.

PEMFCs with various gas flow channel configurations have been presented in the literature. In general, the aim of all of these different pathways is to maximize the area of the reaction surface exposed to the oxygen and hydrogen gas streams and to provide a route for the liquid water produced during the catalytic reaction to exit the fuel cell. The wavelike gas flow channel considered in this study has the additional function of enhancing the gas velocity in the vertical direction to improve the efficiency of the catalytic process.

The heat and mass transfer in both a wavelike gas flow channel and a conventional straight gas flow channel can be modeled with conventional mass conservation, Navier–Stokes, and energy and species conservation equations.[14]

The basic gas transport equations for a general two-dimensional PEMFC are as follows:

TABLE I
Geometric and Physical Parameters in the PEMFC Model

Quantity	Value
Gas channel depth	0.5 mm
Gas channel width	1.0 mm
Gas channel length	100 mm
GDL thickness	0.3 mm
Catalyst thickness	0.05 mm
Membrane thickness	0.125 mm
Porosity of GDL	0.4
Porosity of CL	0.28
Permeability of GDL	1.76×10^{-11} m^2
Permeability of CL	1.76×10^{-11} m^2
Permeability of the membrane layer	1.18×10^{-18} m^2
Tortuosity of GDL	1.5
Tortuosity of CL	1.5
Electronic conductivity of GDL	53 S/m
Electronic conductivity of CL	53 S/m
Inlet temperature	323 K
Operation pressure	1 atm
Anode fuel	H_2, H_2O
Cathode fuel	O_2, N_2
Relative humidity of the anode	100%

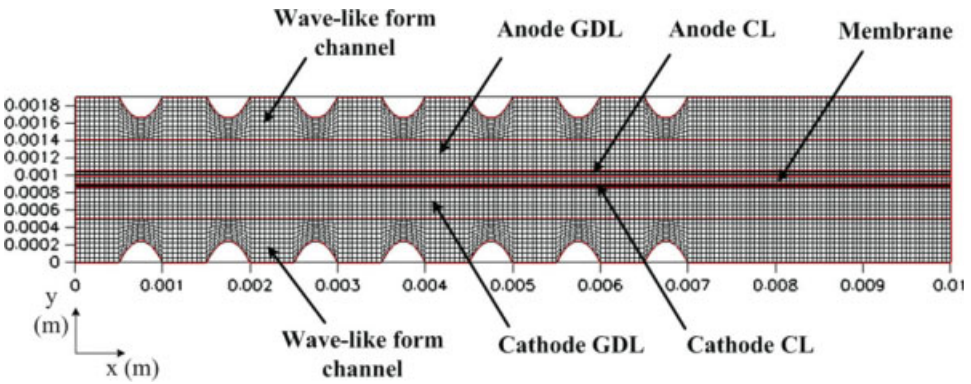

Figure 2 Computational domain of the PEMFC gas flow channel. [Color figure can be viewed in the online issue, which is available at www.interscience.wiley.com.]

Continuity equation:

$$\frac{\partial u}{\partial x}+\frac{\partial v}{\partial y}=0 \tag{1}$$

Momentum equation:

$$\varepsilon_{eff}\left(u\frac{\partial u}{\partial x}+v\frac{\partial u}{\partial y}\right)=-\frac{\varepsilon_{eff}}{\rho}\frac{\partial P}{\partial x}+\upsilon\varepsilon_{eff}\left(\frac{\partial^2 u}{\partial x^2}+\frac{\partial^2 u}{\partial y^2}\right)+S_u \tag{2}$$

$$\varepsilon_{eff}\left(u\frac{\partial v}{\partial x}+v\frac{\partial v}{\partial y}\right)=-\frac{\varepsilon_{eff}}{\rho}\frac{\partial P}{\partial y}+\upsilon\varepsilon_{eff}\left(\frac{\partial^2 v}{\partial x^2}+\frac{\partial^2 v}{\partial y^2}\right)+S_v \tag{3}$$

Energy equation:

$$\varepsilon_{eff}C_p\left(u\frac{\partial T}{\partial x}+v\frac{\partial T}{\partial y}\right)=\frac{k\varepsilon_{eff}}{\rho}\left(\frac{\partial^2 T}{\partial x^2}+\frac{\partial^2 T}{\partial y^2}\right)+S_e \tag{4}$$

Species conservation equation:

$$\varepsilon_{eff}\left(u\frac{\partial C_k}{\partial x}+v\frac{\partial C_k}{\partial y}\right)=D_{k,eff}\left(\frac{\partial^2 C_k}{\partial x^2}+\frac{\partial^2 C_k}{\partial y^2}\right)+S_c \tag{5}$$

Charge conservation equation:

$$\varepsilon_{eff}\left(u\frac{\partial \varphi_e}{\partial x}+v\frac{\partial \varphi_e}{\partial y}\right)=-S_\varphi \tag{6}$$

Table II presents the analytical formulas for the source terms S_u, S_v, S_e, S_c, and S_ϕ in eqs. (2)–(6). In

TABLE II
Analytical Formulas for Source Terms in the Governing Equations

Source term	Flow channel	GDL	CL	Membrane
S_u	0	$-\frac{\upsilon\varepsilon^2}{k_p}u-\frac{\varepsilon_{eff}^3 C_F\rho u}{\sqrt{k_p}}\sqrt{u^2+v^2}$	$-\frac{\upsilon\varepsilon^2}{k_p}u-\frac{\varepsilon_{eff}^3 C_F\rho u}{\sqrt{k_p}}\sqrt{u^2+v^2}$	$-\frac{\upsilon\varepsilon^2}{k_p}u-\frac{\varepsilon_{eff}^2 C_F\rho u}{\sqrt{k_p}}\sqrt{u^2+v^2}$ $+\frac{k_p}{v}Z_f C_H+F\cdot\nabla\phi\frac{\partial u}{\partial x}$
S_v	0	$-\frac{\upsilon\varepsilon^2}{k_p}v-\frac{\varepsilon_{eff}^3 C_F\rho v}{\sqrt{k_p}}\sqrt{u^2+v^2}$	$-\frac{\upsilon\varepsilon^2}{k_p}v-\frac{\varepsilon_{eff}^3 C_F\rho v}{\sqrt{k_p}}\sqrt{u^2+v^2}$	$-\frac{\upsilon\varepsilon^2}{k_p}v-\frac{\varepsilon_{eff}^2 C_F\rho v}{\sqrt{k_p}}\sqrt{u^2+v^2}$ $+\frac{k_p}{v}Z_f C_H+F\cdot\nabla\phi\frac{\partial v}{\partial x}$
S_e	0	$\rho\frac{i_e^2}{k_s^{eff}}$	$\rho j\left[\lvert\eta_{act}\rvert-\frac{T\Delta S}{nF}\right]+\rho\left(\frac{i_m^2}{k_m^{eff}}+\frac{i_e^2}{k_s^{eff}}\right)$	$\rho\frac{i_m^2}{k_m}$
S_c	—	0	$H_2:-\frac{j_a}{2FC_a}$; $O_2:-\frac{j_c}{4FC_c}$; $H_2O:\frac{j_c}{2FC_c}$	$\frac{ZF}{RT}D_{k,eff,H^+}\cdot C_{H^+}\left(\frac{\partial^2\phi}{\partial x^2}+\frac{\partial^2\phi}{\partial y^2}\right)$
S_ϕ	—	0	j	0

these formulas, the parameters ε_{eff}, C_F, k_p, and Z_f denote the effective porosity, the quadratic drag factor, the permeability, and the valence of the species, respectively. Furthermore, $D_{k,eff} = D_k\varepsilon^{\tau_i}$ represents the effective diffusion coefficient of the kth component of the reactant fuel.[15,16] C_k is the mass fraction of the kth component of the reactant fuel, u is the velocity in the x direction, v is the velocity in the y direction, T is the temperature, υ is the viscosity of flow, and ρ is the density.

In the PEMFC, the generation/consumption of the chemical species and the charge transfer are restricted to the CL. Therefore, the source terms in eqs. (5) and (6) can be implemented on the basis of electrochemical kinetics:

$$S_{\mathrm{H_2}} = -\frac{j_{\mathrm{anode}}}{2F} \tag{7}$$

$$S_{\mathrm{O_2}} = -\frac{j_{\mathrm{cathode}}}{4F} \tag{8}$$

$$S_{\mathrm{H_2O}} = -\frac{j_{\mathrm{cathode}}}{2F} \tag{9}$$

where j denotes the transfer current density and F is Faraday's constant. j is derived from the following Butler–Volmer kinetics expressions:

$$j_a = j_{a,ref}\left(\frac{C_{\mathrm{H_2}}}{C_{\mathrm{H_2},ref}}\right)^{1/2} \times \left[\exp\left(\frac{\alpha_a F}{RT}\eta_{act}\right) - \exp\left(-\frac{\alpha_c}{RT}F\eta_{act}\right)\right] \tag{10}$$

$$j_c = -j_{a,ref}\left(\frac{C_{\mathrm{O_2}}}{C_{\mathrm{O_2},ref}}\right) \times \left[\exp\left(\frac{\alpha_a F}{RT}\eta_{act}\right) - \exp\left(-\frac{\alpha_c}{RT}F\eta_{act}\right)\right] \tag{11}$$

where j_a is the transfer current density of the anode, $j_{a,ref}$ is the reference transfer current density of the anode, j_c is the transfer current density of the cathode, R is the universal gas constant, α_a is the transfer coefficient for the reaction of the anode, and α_c is the transfer coefficient for the reaction of the cathode. η_{act} is the surface overpotential and is defined as follows:

$$\eta_{\mathrm{act}} = \varphi_{\mathrm{a,c}} - \varphi_{\mathrm{m}} - \mathrm{V_{OC}} \tag{12}$$

where $\varphi_{a,c}$ and φ_m denote the potentials of the carbon phase and the membrane phase, respectively, in the CL, and V_{OC} is the reference open-circuit potential of the electrode.

The phase potential equation for the potential and current profile is given by:

$$\frac{\partial}{\partial x}\left(\sigma_m\frac{\partial\Phi}{\partial x}\right) + \frac{\partial}{\partial y}\left(\sigma_m\frac{\partial\Phi}{\partial y}\right) = S_j \tag{13}$$

where Φ is the phase potential function and σ_m is the membrane conductivity. It has the following form:[3]

$$\sigma_m(T) = \sigma_m^{ref}\exp\left[1268\left(\frac{1}{303} - \frac{1}{T}\right)\right] \tag{14}$$

where σ_m^{ref} is the reference conductivity of the membrane. It is given by

$$\sigma_m^{ref} = 0.005139\lambda - 0.00326 \tag{15}$$

$$\lambda = \begin{Bmatrix} 0.043 + 17.81\cdot a & \text{for} \quad 0 < a \le 1 \\ -39.85\cdot a^2 + 36.0\cdot a^3 & \\ 14 + 1.4\cdot(a-1) & \text{for} \quad 1 \le a \le 3 \end{Bmatrix} \tag{16}$$

where λ is the water content of the membrane and a is the water activity. It is defined as follows:

$$a = \frac{x_{\mathrm{H_2O}}P}{P_{sat}} \tag{17}$$

where P is the pressure and P_{sat} is the saturation pressure. In eq. (17), P_{sat} varies with the temperature and can be determined directly from thermodynamic tables or from the following empirical expression:

$$P_{sat} = 10^{-2.1794+0.02953T-9.1837\times10^{-5}T^2+1.4454\times10^{-7}T^3} \tag{18}$$

BOUNDARY CONDITIONS

The governing equations for the current PEMFC model are elliptic, partial differential equations, and hence boundary conditions are required for all of the boundaries in the computational domain. Because of the conjugated nature of the current problem, the gas flow channel surfaces are included within the solution domain and are treated as a particular type of fluid.

The boundary conditions are as follows:

1. Gas flow channel:
   Anode inlet:

$$\begin{aligned} &u = u_{in}, T = T_{in} \\ &v = 0, C_{\mathrm{H_2}} = C^a_{\mathrm{H_2},in}, C_{\mathrm{H_2O}} = C^a_{\mathrm{H_2O},in} \end{aligned} \tag{19}$$

Cathode inlet:

$$u = u_{in}, T = T_{in}$$
$$v = 0, C_{O_2} = C^c_{O_2,in}, C_{N_2} = C^c_{N_2,in} \quad (20)$$

Interface between the gas flow channel walls and CL:

$$u = v = \frac{\partial C_k}{\partial x} = 0 \quad (21)$$

2. Gas flow channel outlet:

$$\frac{\partial u}{\partial x} = \frac{\partial v}{\partial x} = \frac{\partial T}{\partial x} = 0 \quad (22)$$

3. Upper surface:
Anode gas channel:

$$u = v = 0 \quad (23)$$
$$T_{\text{surface}} = 298 \text{ K} \quad (24)$$

4. Lower surface:
Cathode gas channel:

$$u = v = 0 \quad (25)$$
$$T_{\text{surface}} = 298 \text{ K} \quad (26)$$
$$T_{in} > T_w \quad (27)$$

where T_{in} is the inlet temperature, T_{surface} is the surface temperature, and T_w is the wall temperature.

NUMERICAL METHOD

Figure 3 presents a flow chart of the current numerical modeling procedure. In this study, the simulations are performed with the commercial CFD-RC software package, which discretizes the mass, momentum, energy, and species concentration equations with the finite-volume SIMPLEC (semi-implicit method for pressure-linked equations consistent) method.[17] The various models in CFD-ACE are fully described in ref. 18. In the simulations, it is assumed that the inlet section of the channel is fully developed hydrodynamically. Hence, a fully developed velocity profile for rectangular ducts is imposed. Additionally, a forced convection regime is imposed within the computational domain, and the Navier–Stokes equations are solved under laminar assumptions. Before the simulations, a parametric study was performed to identify a suitable grid mesh for accurately modeling the thermal and velocity gradients near the walls to provide detailed insights into the electrochemical reaction and mass transport phenomena in the PEMFC. A spatial resolution of 200 mesh × 40 mesh was found to be sufficient, with a fine mesh size used throughout the computational domain. In the simulations, the iterative computations were terminated once the value of the residues fell to less than 10^{-6}. The computations were performed with a personal computer with a 3.2-GHz Intel Pentium 4 central processor unit, 1 GB of DDR RAM, and the Windows XP operating system.

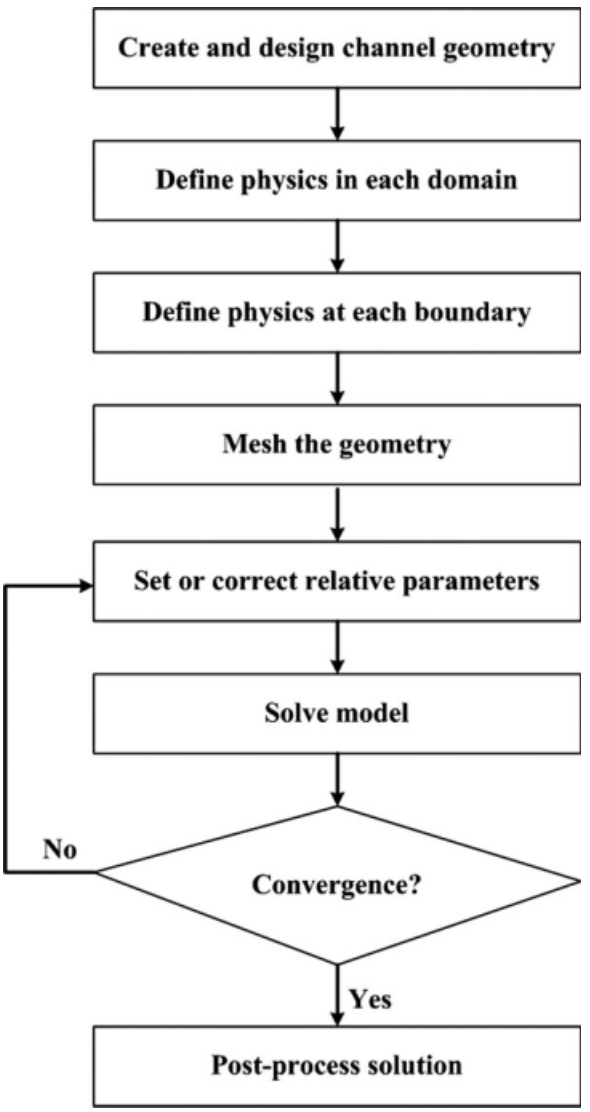

Figure 3 Flow chart of the modeling and simulation procedure.

RESULTS AND DISCUSSION

Velocity field

The transport phenomena in the gas flow channel and GDL of a PEMFC have a fundamental effect on the fuel cell performance. The fluid flow in the wavelike gas flow channel has an axial flow velocity

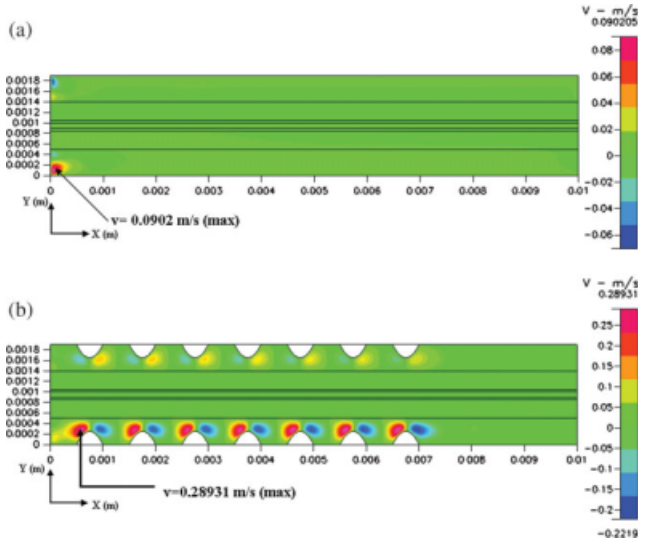

Figure 4 Velocity field in the y direction of the gas flow channels: (a) straight geometry and (b) wavelike geometry. [Color figure can be viewed in the online issue, which is available at www.interscience.wiley.com.]

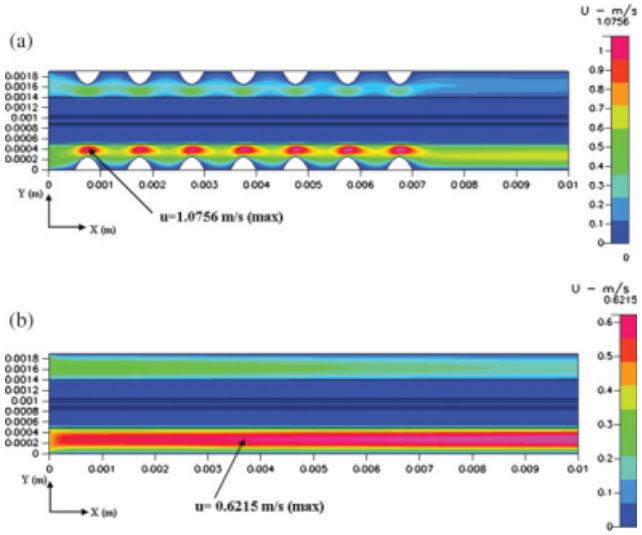

Figure 5 Velocity field in the x direction of the gas flow channels: (a) wavelike geometry and (b) straight geometry. [Color figure can be viewed in the online issue, which is available at www.interscience.wiley.com.]

and a flow vector in the y direction. Figure 4(a) shows the vertical (i.e., y direction) velocity profile in a conventional straight gas flow channel for laminar flow with a PEMFC operating potential of 0.6 V, a cathode gas flow inlet velocity of 0.4 m/s, and an anode gas flow inlet velocity of 0.2 m/s. Meanwhile, Figure 4(b) illustrates the vertical velocity profile in the wavelike flow channel under the same conditions. It is apparent that the periodic wavelike structure of the proposed gas flow channel increases the velocity of the flow in the vertical direction. Hence, the catalytic reaction in the CL is enhanced, and the performance of the PEMFC is correspondingly improved. Figure 5 shows the distributions of the axial flow velocity in the wavelike gas flow channel and the straight gas flow channel. The local maximum velocities are indicated in both cases. In general, the fuel side (anode) has a lower velocity than the air side (cathode) because the fuel has a smaller stoichiometric coefficient. Furthermore, it is apparent that the velocity is higher in the wavelike channel than in the straight channel. The maximum velocity occurs in the region immediately above the crests of the profiled surface. The velocity in the wavelike channel is higher than that in the straight channel because the constricted channel area above each crest introduces a nozzle-type effect that accelerates the flow. In general, the pressure drop characteristics are unaffected by the flow direction. Figures 4 and 5 show that for a cathode gas flow inlet velocity of 0.4 m/s and an anode gas flow inlet velocity of 0.2 m/s, the maximum y-direction velocity in the wavelike channel is 0.289 m/s, and the maximum x-direction velocity is 1.0756 m/s. Furthermore, the figures show that the wavelike form of the gas channel causes the axial velocity to decrease in the valley regions of the channel. Hence, the provision of fuel to the reaction layer is increased. Figures 4 and 5 also show that the wavelike form flow channel induces a strong convection force along the reaction surface. This further increases the supply of the reactant gases to the CLs and also improves the removal of the reaction byproducts from the PEMFC. Thus, the performance of the fuel cell is significantly improved, particularly at higher current densities.

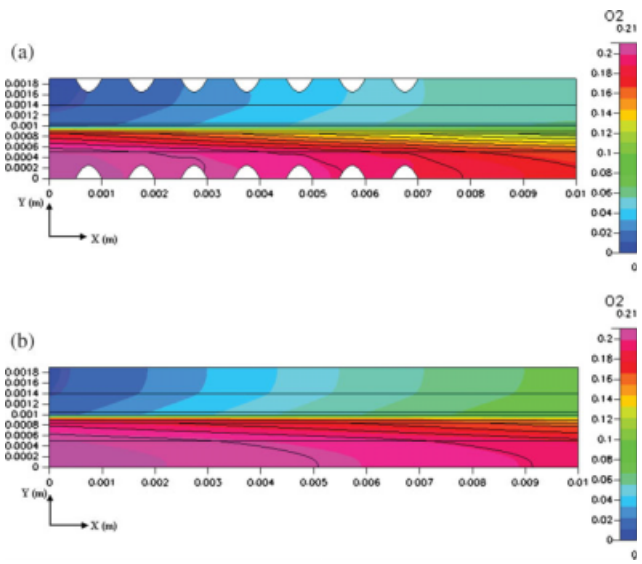

Figure 6 Oxygen concentration distribution in the gas flow channels at a cell voltage of 0.6 V: (a) wavelike geometry and (b) straight geometry. [Color figure can be viewed in the online issue, which is available at www.interscience.wiley.com.]

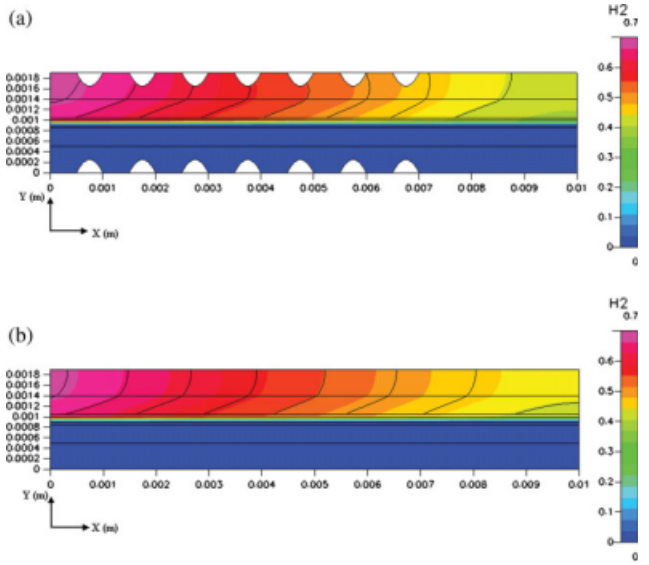

Figure 7 Hydrogen concentration distribution in the gas flow channels at a cell voltage of 0.6 V: (a) wavelike geometry and (b) straight geometry. [Color figure can be viewed in the online issue, which is available at www.interscience.wiley.com.]

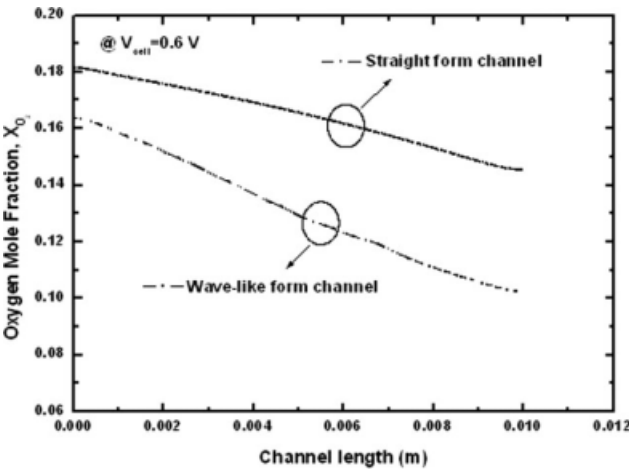

Figure 8 Oxygen molar fraction profiles in cathode CLs of the gas flow channels at a cell voltage of 0.6 V.

Concentration distribution

Figures 6 and 7 show the oxygen and hydrogen concentrations in the wavelike and straight gas flow channels. In both figures, the cathode overpotential is 0.6 V, and the color-coded scale indicates the normalized concentration of the two gases. Figure 6 shows that the oxygen concentration in the wavelike channel decreases slightly along the axial direction. Furthermore, it is observed that the oxygen concentration varies significantly in the GDL region, particularly near the reaction surface. By contrast, in the straight gas flow channel, the oxygen concentration near the reaction surface is relatively uniform. The greater variation in the oxygen concentration in the wavelike gas channel is the result of the forced convection effect in the diffusion layer, which permits more oxygen to diffuse through the layer, thereby enhancing the chemical reaction. By contrast, the straight gas flow channel achieves only a limited oxygen and hydrogen transfer rate in the reaction surface region because transport is achieved by diffusion only.

Figure 8 shows the oxygen concentration distributions in the wavelike and straight form gas flow channels for a cell voltage of 0.6 V. The oxygen molar fraction decreases along the flow direction as a result of absorption in the CL. Furthermore, it is apparent that the oxygen consumption is higher in the wavelike channel than in the straight channel.

Temperature field

Figure 9 shows the temperature distributions in the wavelike gas flow channel and straight gas flow channel for a cathode gas inlet velocity of 0.4 m/s and an anode gas inlet velocity of 0.2 m/s. The wavelike channel results in a lower and more uniform temperature distribution throughout the channel. In other words, the wavelike gas flow channel improves the heat-transfer performance of the PEMFC and reduces the cell reaction temperature. In general, the improvement obtained in the single-phase convective heat-transfer performance in the gas flow channel may be the result of an increased flow interruption, a reduction in the thermal boundary layer, or an increased velocity gradient near the GDL boundary.

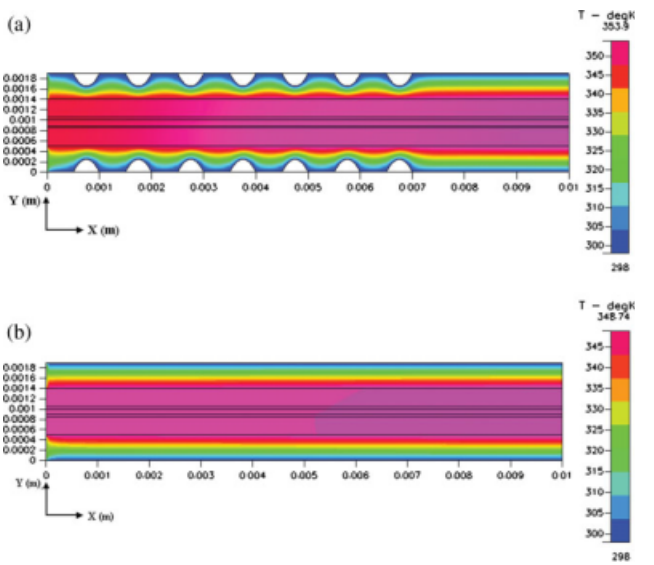

Figure 9 Temperature field in the gas flow channels at an inlet temperature of 323 K (50°C): (a) wavelike geometry and (b) straight geometry. [Color figure can be viewed in the online issue, which is available at www.interscience.wiley.com.]

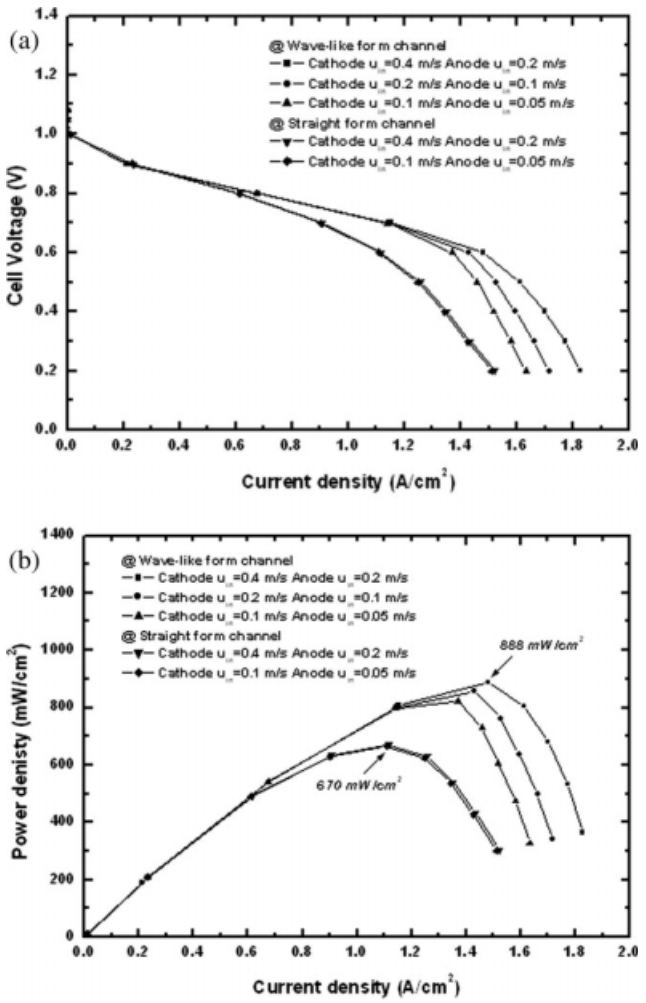

Figure 10 (a) Polarization curve and (b) power density curve in the gas flow channels for various inlet velocity conditions.

Polarization curve

The polarization characteristics of a PEMFC provide a convenient means of evaluating the performance of fuel cells with different gas flow channel configurations. Figure 10 shows the polarization and power density curves of PEMFCs with wavelike and straight gas flow channels, respectively. For an oxygen inlet velocity of 0.4 m/s and a hydrogen inlet velocity of 0.2 m/s, the PEMFC with a wavelike gas channel yields a higher cell voltage and power density. For an oxygen inlet velocity of 0.1 m/s and a hydrogen inlet velocity of 0.05 m/s, both PEMFCs have a poorer performance. However, the electrical performance of the PEMFC with the wavelike gas flow channel is still better than that of the PEMFC with the conventional straight channel because the wavelike surface increases the supply of oxygen to the reaction layer. Figure 10 also shows that the power density of the PEMFC with the wavelike gas flow channel is approximately 32.5% higher than that of the PEMFC with the straight channel. This result demonstrates that the wavelike surface of the flow channel changes the transport of the reactant gas to the CL surface from a diffusion mechanism to a convection mechanism, resulting in a significantly improved electrical performance.

CONCLUSIONS

In this study, we have developed a two-dimensional computational model to study the transport phenomena in PEMFCs with wavelike gas flow channels and conventional straight gas flow channels. The heat-transfer performance and gas flow velocity characteristics of the two channel geometries have been examined. The results have shown that compared to the conventional gas flow channel, the wavelike channel provides a significantly improved convective heat-transfer performance and a higher gas flow velocity, which in turn improves the efficiency of the catalytic reaction. Furthermore, compared with the PEMFC with conventional straight gas flow channels, the PEMFC with wavelike gas flow channels has improved current density and polarization characteristics.

NOMENCLATURE

Symbols

a	water activity
C	mass fraction
C_F	quadratic drag factor
C_p	constant pressure specific heat (kJ/kgK)
D	mass diffusion (m^2/s)
F	Faraday's constant (96,485 C/mol)
i_e	current density (A/m^2)
i_m	ionic current density (A/m^2)
j	transfer current density (A/m^3)
k	thermal conductivity (w/mk)
k_c	condensation rate constant (1/s)
k_e	evaporation rate constant (1/atm s)
k_m^{eff}	effective ionic conductivity of the membrane (S/cm)
k_s^{eff}	elective electric conductivity of the gas diffusion layer (S/cm)
k_p	permeability (m^2)
M	molecular weight (kg/mol)
n	charge number of the sulfonic acid ions
P	pressure (atm)
P_{sat}	saturation pressure
R	universal gas constant (8.314 J/mol k)
S	source term
T	temperature (K)
u	velocity in the x direction (m/s)
v	velocity in the y direction (m/s)
V	operating voltage (V)

V_{OC} open-circuit potential of the electrode
X_{H_2O} humidity ratio
Z_f species valence

Greek symbols

α transfer coefficient for the reaction
β coefficient of thermal expansion
ε porosity
η_{act} activation overpotential (V)
λ water content of the membrane
ρ density (kg/cm^2)
σ ionic conductivity (1/Ω m)
τ tortuosity
υ viscosity of flow (kg/m s)
Φ phase potential (V)

Subscripts

a anode
c cathode
CL catalyst layer
e energy
eff effective
GDL gas diffusion layer
h_1 gas flow channel height
h_2 gas diffusion channel height
in inlet
k *k*th component of the fuel reactant
m membrane phase
mem membrane
out outlet, outer
ref reference
w wall
x *x* direction
y *y* direction

References

1. Bernardi, D. M.; Verbrugge, M. W. AIChE J 1991, 37, 1151.
2. Bernardi, D. M.; Verbrugge, M. W. J Electrochem Soc 1992, 139, 2477.
3. Springer, T. E.; Zawodzinski, T. A.; Gottesfeld, S. J Electrochem Soc 1991, 136, 2334.
4. Nguyen, T. V.; White, R. E.; Water, A. J Electrochem Soc 1993, 140, 2178.
5. Meng, H.; Wang, C. Y. J Electrochem Soc A 2004, 151, 358.
6. Kuo, J. K.; Chen, C. K. J Power Sources 2006, 162, 207.
7. Kuo, J. K.; Chen, C. K. J Power Sources 2006, 162, 1122.
8. Hwang, J. J.; Chao, C. H.; Ho, W. Y.; Chang, C. L.; Wang, D. Y. J Power Sources 2006, 153, 130.
9. Gurau, V.; Liu, H.; Kakac, S. AIChE J 1998, 46, 2410.
10. Um, S.; Wang, C. Y.; Chen, K. S. J Electrochem Soc 2000, 147, 4485.
11. Wang, Z. H.; Wang, C. Y.; Chen, K. S. J Power Sources 2001, 94, 40.
12. Mazumder, S.; Cole, J. V. J Electrochem Soc 2003, 150, 1510.
13. Hu, G.; Fan, J.; Chen, S.; Liu, Y.; Cen, K. J Power Sources 2004, 136, 1.
14. Wang, Y.; Wang, C. Y. J Electrochem Soc A 2005, 152, 445.
15. Wang, C. Y. Chem Rev 2004, 104, 4727.
16. Lee, C. I.; Chu, H. S. J Power Sources 2006, 161, 949.
17. Patankar, S. V. Numerical Heat Transfer; Hemisphere: Washington, DC, 1980.
18. CFD-ACE (U)^{TM} User Manual, Version 2002; CFD Research: Huntsville, AL, 2002.